Influence and Propagation of Axial Power Distribution Varying on Thermal-Hydraulic Characteristics in a Rod Bundle

Zixuan Wang[a,b], Yi Meng[a,b], Yan Wang[a,b*]
[a]Institute of Nuclear and New Energy Technology (INET), Tsinghua University, Beijing 100084, China
[b]Key laboratory of advanced reactor engineering and safety, Ministry of Education, Tsinghua University, Beijing 100084, China
* wangyanfcw@tsinghua.edu.cn

Abstract: The reactor operation performance and safety are strongly associated with its thermal-hydraulic design. It is of great significance to thoroughly estimate the key thermal-hydraulic parameters (e.g., critical heat flux) during the reactor design and safety analysis. The uneven and time-varying power distribution during operation can result in various local thermal-hydraulic behaviors, which make it rather difficult to get a clear picture of how the thermal-hydraulic characteristics in each subchannel are affected by the axial power shape varying of certain fuel rods in a fuel assembly. In this paper, a 5×5 rod bundle was taken as the research object, and a set of cases with various boundary conditions cases was designed to carefully research this phenomenon. These cases were modeled and analyzed by the subchannel code CTF. Using the uniform axial power distribution (APD) as the baseline, comparative analyses were conducted by altering the central rod APD (from uniform to cosine, inlet or outlet peak distribution). Furthermore, the effect of radial power distribution was taken into consideration to investigate whether the APD impact would be amplified or diminished. The results show that under various central rod APDs, the thermal-hydraulic parameters like the void fraction, mass flux in central subchannels are changed. The MDNBR value of central rod might be below the safety criterion under certain APD pattern while its position notably shifts towards the power peak. Nevertheless, such effect is non-global since the parameter variations in side or corner subchannel are neglectable. Additionally, the impact of central rod APD varying almost remains stable as its power increases. The relative variation of coolant mass flux in subchannels not adjacent to central rod are within 1.6%. Moreover, the central rod APD varying has little impact on other solid region with the maximum cladding temperature variation of other rods below 0.5°C.

Keywords: Thermal hydraulics, Reactor safety, Power distribution, Subchannel analysis.

1. INTRODUCTION

In a light water reactor, the local coolant behaviors are closely associated with the local power and local geometries. The full understanding of the relationship and interaction between the two is of great significance, which could supply reactor design and safety analysis with accurate inputs [1]. However, the power distributions of fuel rods in reactor assemblies are usually non-uniform (both axial and radial) and time-varying (during the fuel life-cycle). In the open and narrow subchannel geometry, the axial power distribution (APD) changing of fuel rod with a high-level heated power can lead to the obvious variations of thermal-hydraulic (T/H) parameters in neighboring subchannels. In addition, such effect may propagate core-wide by the strong dynamic interaction among subchannels [2]. Hence, it is of necessity and challenges to get a clear picture of the power distribution impact on T/H parameters and its propagation in subchannels.

In recent years, the details of the local flow fields, convective and boiling heat transfers, flow induced vibrations, inter-subchannel mixings, potential interactions among subchannels, as well as flow regime transitions under non-uniform power distributions have been investigated in both experimental and numerical ways.

Among numerous T/H phenomena, critical heat flux (CHF) has attracted extensive research interest since it serves as the criterion of reactor safety limits. Yang et al. [3] conducted rod bundle experiments with uniform and non-uniform APD to discuss the applicability of using rod bundle CHF data with uniform APD for CHF correlation development of light water reactors with non-uniform APD. Based on the liquid sublayer dryout mechanism, Liu et al. [4] proposed an improved CHF prediction model for non-uniform APD, where the local T/H characteristic at boiling crisis point was determined by considering upstream non-uniform heating power. The CHF under different types of APD were calculated and compared with the experimental data. Zhu et al.

[5] simulated the distribution of local two-phase thermal hydraulic parameters and CHF in a radially non-uniformly heated rod assembly. The researchers found that as the heating power increases from 0 to the critical level, the quality and void fraction affected two-phase velocity, which determined the distribution of mass flow rate in subchannels. Wang et al. [6] investigates the effect of power peak value and location on system instability in rod bundle. The results showed that the backward shift and the increase of and power peak could prolong the single-phase region, thereby stabilizing the system. With the intention of analyzing the power distribution impact on the thermionic reactor's thermal-hydraulic and thermoelectric characteristics, Dai et al. [7] developed a three-dimensional computational fluid dynamic (CFD) model of a full-scale thermionic space reactor core. The T/H analyses indicated that compared with uniform APD, the maximum temperature in each component of the reactor core was much higher under cosine APD, while the APD has little effect on the output power and coolant temperature distribution.

Although much work has been done on the prediction of CHF under non-uniform APD, few studies focus on the influences of APD changing on the thermal-hydraulic behaviors in subchannels and how such effect propagates. In this paper, a 5 × 5 rod bundle was modeled and several patterns of APD were designed to analyze the diffusion of the power distribution impact on the subchannel thermal-hydraulic characteristics. To study whether a high heated power level would amplify the effect propagation in the rod bundle, a preliminary sensitivity analysis was also conducted. Moreover, the effects of axial power peak shifting and flattening on thermal-hydraulic parameters were investigated.

2. DESCRIPTION OF RESEARCH OBJECTIVE

2.1. Nonuniform heated rod bundle model

The nonuniform heating power in a fuel assembly can result in various and complicated T/H characteristics in subchannels, as shown in Figure 1. In particular, the narrow and different geometries of subchannels, as well as the intense interaction among the open subchannel structure, make it rather challenging to obtain an accurate analytical expression of the power distribution impact on T/H characteristics in subchannels.

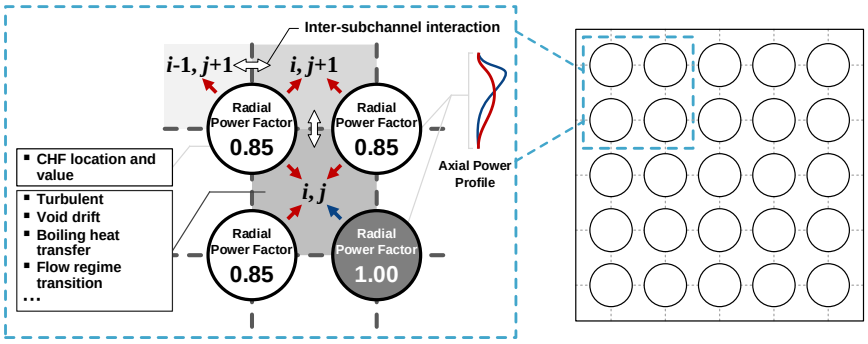

Figure. 1 The Impact of Various Power Distribution on Thermal-hydraulic Characteristics in Subchannels

As an attempt to analyze such effect, this paper proposes a both axially and radially non-uniform heated rod bundle with different boundary conditions to cover various operating conditions. Meanwhile, considering the effect of subchannel location and geometry, a 5×5 rod bundle is selected as a representative example. The geometric and structural parameters derive from NUPEC PWR Subchannel and Bundle Test (PSBT) 5×5 rod bundle test assembly, which will be introduced in section 4.1.

Table 1. Metrics of Power Distribution Impact

Parameter	Thermal-hydraulic Phenomenon
Mass flux	The match between the coolant flow and heating power affects the reactor efficiency and safety
DNBR (MDNBR)	Measures the margin to critical heat flux
Maximum Cladding temperature	Affects the heat transfer from the fuel pellets to the reactor coolant, coolant boiling on surface and critical heat flux
Void fraction	Provides an insight into the phase distributions (gas/vapor, liquid), which affects the heat transfer, flow dynamics and stability, etc.

2.2. Metrics of power distribution impact on thermal-hydraulic characteristics

From the perspective of operation safety and performance of reactor, a set of T/H parameters that people mainly concerned about have been selected as the metrics of the power distribution impact. Table. 1 presents these metrics and the T/H phenomena that they characterize.

3. NUMERICAL METHODS

3.1. Subchannel analysis code CTF

After years of development, the subchannel analysis codes that can reflect the two-phase flow and heat transfer phenomena in the rod bundle have become a widely acknowledged approach to reactor T/H analysis. Researchers have developed corresponding subchannel codes for different types of nuclear reactors, for instance, COBRA series codes for light water reactor [8], ASSERT for heavy water reactor (CANDU) [9], SACOS-Na for sodium fast reactor [10] and so on. Given that this study focuses on the T/H analysis under PWR operating conditions, the non-uniform heated rod bundle in this study is modeled by the subchannel code CTF, which is an improved descendent of COBRA/TRAC code [11] and has undergone sufficient verification and validation (V&V) work in the last decade [12].

The CTF code employs a two-fluid model that considers three separate fluid fields (liquid film, entrained droplets, and vapor). Assuming that the liquid and droplet fields are in thermal equilibrium, the code solves nine coupled conservation equations: mass conservation of the liquid, vapor, and droplets; momentum conservation of the liquid, vapor, and droplets; and energy conservation of the liquid, vapor, and solids. A form of the Semi-Implicit Method for Pressure-Linked Equations (SIMPLE) is applied to numerical solution in CTF. Eq. 1-3 gives the generalized form of mass, momentum, energy conservation equations [11]:

$$\frac{\partial}{\partial t}\left(\alpha_k \rho_k\right)+\nabla\cdot\left(\alpha_k \rho_k \vec{V}_k\right)=L_k+M_e^T \tag{1}$$

$$\frac{\partial}{\partial t}\left(\alpha_k \rho_k \vec{V}_k\right)+\nabla\cdot\left(\alpha_k \rho_k \vec{V}_k \vec{V}_k\right)=\alpha_k \rho_k \vec{g}-\alpha_k \nabla P+\nabla\cdot\left[\alpha_k\left(\tau_k^{ij}+T_k^{ij}\right)\right]+\vec{M}_k^L+\vec{M}_k^d+\vec{M}_k^T \tag{2}$$

$$\frac{\partial}{\partial t}\left(\alpha_k \rho_k h_k\right)+\nabla\cdot\left(\alpha_k \rho_k h_k \vec{V}_k\right)=-\nabla\cdot\left[\alpha_k\left(\vec{Q}_k+\vec{q}_k^T\right)\right]+\Gamma_k h_k^i+q_{wk}'''+\alpha_k \frac{\partial P}{\partial t} \tag{3}$$

Where subscript k denotes the phase kind (liquid film, vapor, or entrained droplet); α_k, ρ_k, $\vec{V}_k$, h_k represent the void fraction, density, velocity, enthalpy of *k*-phase respectively. On the right side of Eq. 1, the first term denotes the mass transfer into or out of k -phase, while the second is the mass transfer in the mesh cell due to turbulent mixing and void drift. On the right side of Eq. 2, the terms represent: gravitational force, pressure force, viscous and turbulent shear stress, momentum source/sink due to phase change and entrainment, interfacial drag forces, and momentum transfer due to turbulent mixing. The terms on the right side of Eq. 3 stand for: *k*-phase conduction and turbulence heat flux, energy transfer due to phase change, volumetric wall heat transfer, and the pressure work term.

The conservation equations contain several terms due to physical phenomena like void drift and turbulent mixing, which are dubbed “closure terms”. These terms must be defined to complete the solution. The closure terms and corresponding modeling choices in this study are outlined as below. A more detailed discussion of the closure terms can be found in the CTF theory manual [13].

- CTF adopts the Lahey and Moody approach to model turbulent mixing and void drift phenomena. Here, the single-phase mixing coefficient is derived using an empirical correlation by Rogers and Rosehart. The two-phase turbulent mixing is according to the Beus’ model [13].

- For forced convection heat transfer, considering the pressure conditions and correlation applicability range, the Thom model is utilized.

- The interfacial drag force per unit volume between any two fields is assumed to be a function of the relative velocity between both fields, and the interfacial drag coefficients depend on flow regimes and bubble size:

$$\begin{aligned} &\text{Between continuous liquid and vapor: } \tau_{I,vap\_liq} = K_{I,vap\_liq} U_{vap\_liq} \\ &\text{Between entrained liquid and vapor: } \tau_{I,vap\_ent} = K_{I,vap\_ent} U_{vap\_ent} \end{aligned} \quad (4)$$

- Wall friction is approximated using Eq. 5, considering the PSBT rod bundle material and structure:

$$\lambda = \max\left(1.691 Re^{-0.43}, 0.117 Re^{-0.14}\right) \quad (5)$$

- Noncondensible gases and the droplet phase are not modeled. Given the assumption that the unheated section at the top of the rod bundle is adiabatic, it is not explicitly modeled in the code. Since the outer casing of the experiment facility is assumed to be adiabatic, there is no heat loss to the environment.

3.2. Process of power distribution impact evaluation

In the current work, the analysis of the power distribution impact can be divided into three stages as follows. Figure 2 depicts the details of the evaluation process.

***Model validation*:** Benchmark the simulation results against the experimental data and reference numerical data for given exercises in PSBT benchmark.

***Influence of axial power shape*:** Design several typical APDs, including cosine, uniform, inlet and outlet peak distribution; apply these APDS to the certain rods and analyze the parameter variation in each subchannel.

***Comprehensive evaluation of axial and radial power distribution impact*:** Change the power level of the heated rods with various APDs to investigate whether the axial power distribution impact would be expanded or shrunk.

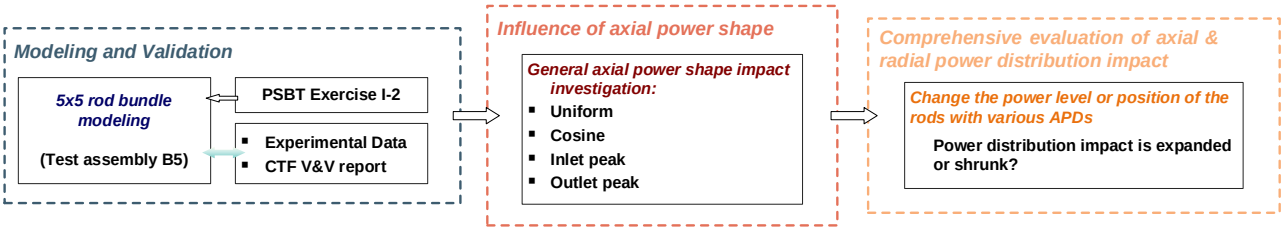

Figure. 2 Process of Evaluating the Power Distribution Impact on Subchannel Thermal-Hydraulic Characteristics

4. RESULTS AND DISCUSSION

4.1. Model validation

The nonuniform heated rod bundle in this study is modeled using data from a PSBT 5×5 rod bundle (Test assembly B5), whose main parameters are listed in Table. 2. The NUPEC PSBT benchmark is a critical resource that provides essential data for the development and validation of T/H solvers.

To ensure the follow-up analysis is credible, a validation study of the numerical model has been conducted. The numerical results are compared with the existing data, including the PSBT experimental data and the simulation data from the CTF V&V report [12].

Figure 3(a) shows that the predictions of quality are in good consistency with the experimental data at different elevations (lower, middle, and upper elevations; LE, ME, UE). It can be seen from Figure 3(b) that the void fraction results are almost identical with the calculated values published on the CTF V&V report. The dashed lines depict the experimental uncertainty. The calculated results are basically within the dashed boundaries, and agree well with the experimental data. Moreover, the root-mean-square error (RMSE) is utilized as a comparison metric to indicate the magnitude of errors between calculated and measured results, as shown in

Eq. 6. Table. 3 gives the detailed RMSE results, and the general RMSE is acceptable. In summary, the correctness of 5x5 rod bundle modeling has been confirmed.

$$\mathrm{RMSE} = \sqrt{\frac{1}{N}\sum_{i=1}^{N}\left(X_{\mathrm{CTF},i} - X_{\mathrm{exp},i}\right)^2} \tag{6}$$

Table 2. Main Parameters of PSBT Test Assembly B5

Item	Value
Number of heated rods	25 (5×5 rod array)
Heated rod outer diameter (mm)	9.50
Thimble rod outer diameter (mm)	-
Heated rods pitch (mm)	12.60
Axial heated length (mm)	3658
Flow channel inner width (mm)	64.9
Radial power profile	0.85:1.00
Axial power profile	uniform
Number of mixing vane spacers (pressure loss coefficient)	7 (1.00)
Number of non-mixing vane spacers (pressure loss coefficient)	2 (0.70)
Number of simple spacers (pressure loss coefficient)	8 (0.40)

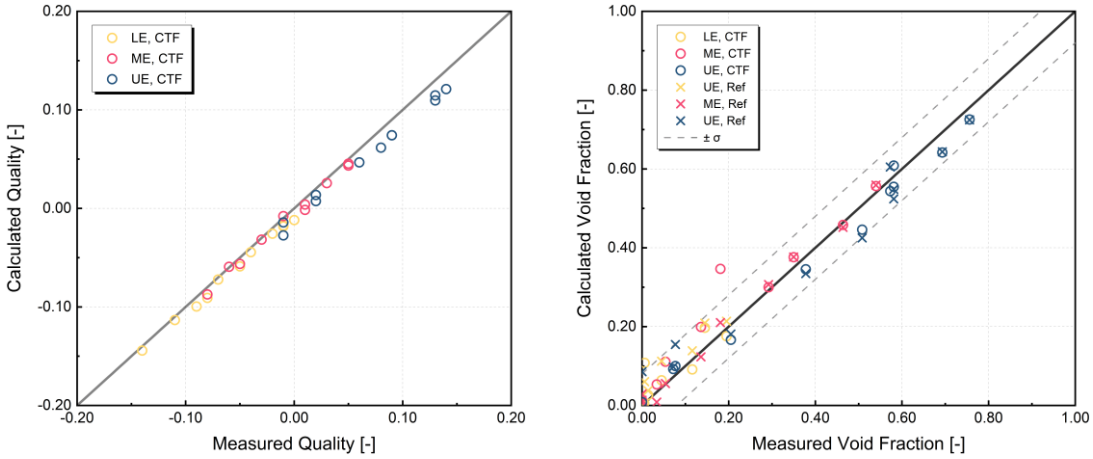

(a) (b)

Figure 3. Comparison of PSBT Test Series 5 Results: (a) Thermal Equilibrium Quality; (b) Void Fraction

Table 3. Error comparison between simulation results and reference

RMSE	Simulation results	Reference
Lower Elevation	0.0364	0.0340
Middle Elevation	0.0575	0.0308
Upper Elevation	0.0346	0.0595

4.2. Influence of APD patterns on T/H parameters

In this section, four typical patterns of APD are designed to investigate the power distribution impact on T/H characteristics in a systematic way, including cosine, uniform, inlet peak, and outlet peak distribution, as shown in Figure 4a. Figure 4b illustrates the radial power distribution (type I) and the indices of subchannels and heating rods. To cover a range of operating conditions, a series of cases are designed, from high pressure/inlet mass flux/heating power to low pressure/inlet mass flux/heating power, as listed in Table. 4.

The APD of rods in the bundle are all originally uniform. By changing the axial power profile of central rod, the single impact of APD varying on subchannel T/H characteristics can be captured. Figure 5-10 present the comparison of local void fraction and mass flux in rod bundle with different central rod APDs.

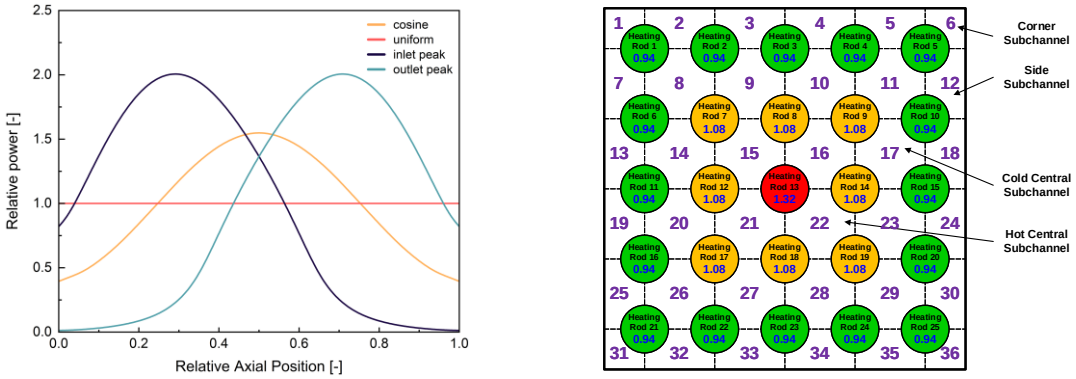

(a) (b)

Figure 4. (a) Four APD Patterns; (b) Schematic of Subchannel Division and Radial Power Distribution

Table 4. Error comparison between simulation results and reference

Case	Press [bar]	W_{in} [10^6 kg/hr·m^2]	Power [kW]	T_{in} [°C]	Radia Power distribution
1 I	155.0	11.80	3000	268.0	I
2 I	120.0	8.80	2650	236.0	I
3 I	80.0	5.60	2000	230.0	I

It can be observed from Figure. 5 that under various APDs, the axial void distribution in adjacent channels exhibits significant differences. For the outlet peak distribution of the central rod, due to the higher local heat flux at the upper elevation, the void generated under subcooled boiling gradually increases and drifts upwards, resulting in a significantly higher void fraction at the outlet compared to the inlet peak and cosine distribution. What's more, a variation on the void fraction in cold central subchannel (e.g., subchannel 8, 9) has been observed, which could be attributed to the joint effort of central rod varying and subchannel interaction. The results of Case 1 I is similar to those of Case 2 I However, under low pressure and low flow conditions (Case 3 I, Figure 6), due to the low subcooling degree, a large number of voids have already appeared in each channel. At this time, the difference in local heating power at the top will not have a significant impact on the void distribution.

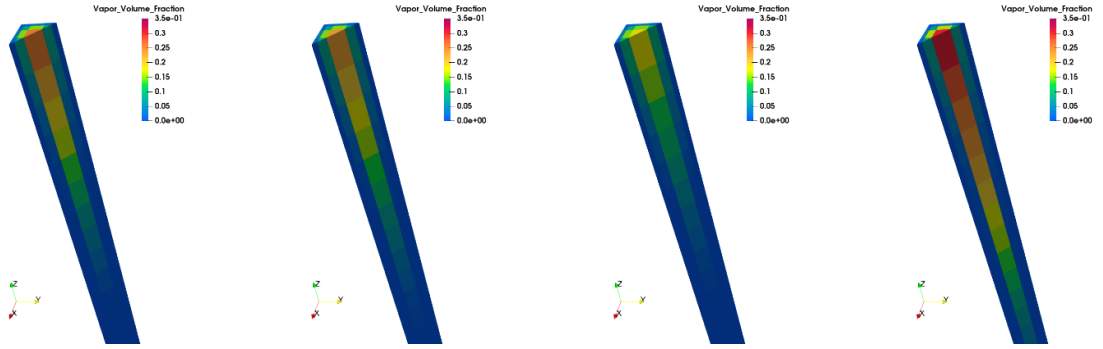

Uniform Cosine Inlet Peak Outlet Peak

Figure 5. Local void fraction in rod bundle with various central rod APDs in Case 2 I

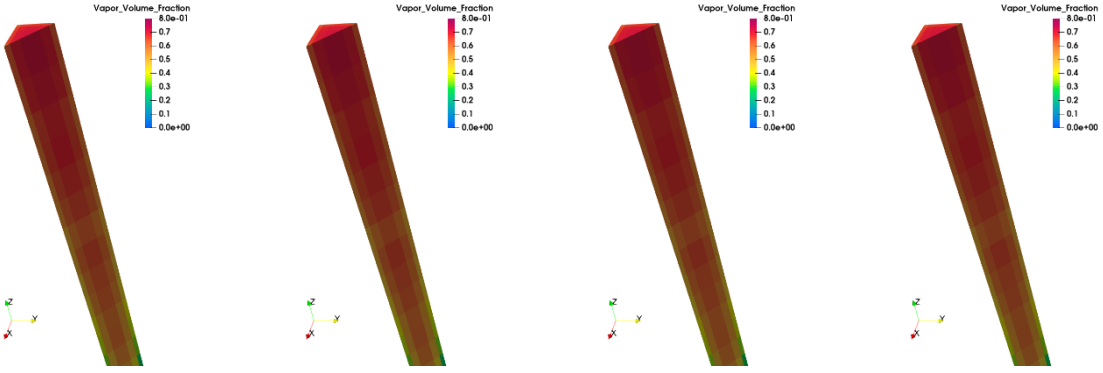

Uniform Cosine Inlet Peak Outlet Peak

Figure 6. Local void fraction in rod bundle with various central rod APDs in Case 3 I

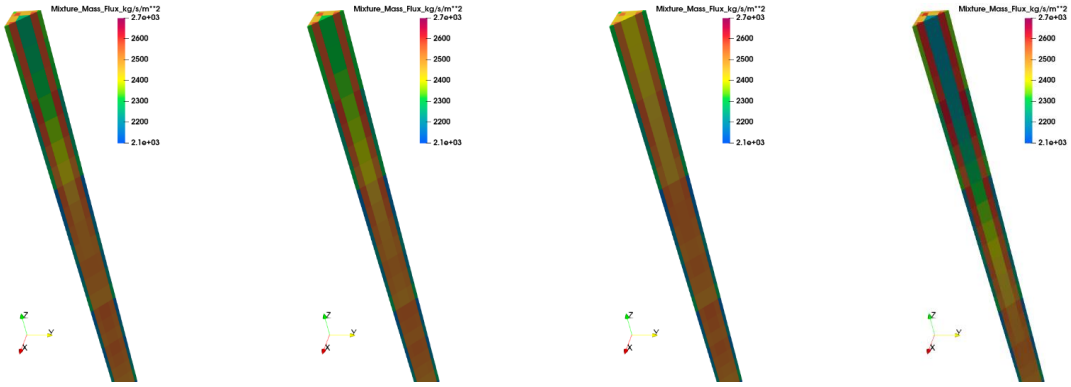

Uniform Cosine Inlet Peak Outlet Peak

Figure 7. Local mass flux in rod bundle with various central rod APDs in Case 2 I

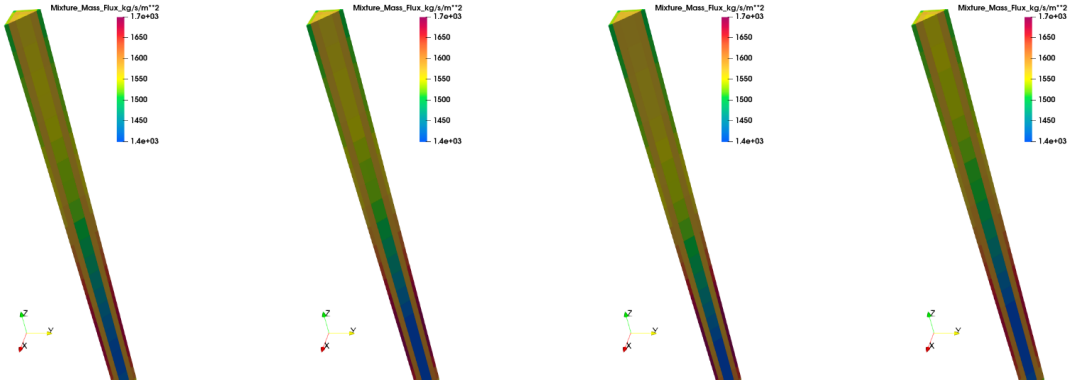

Uniform Cosine Inlet Peak Outlet Peak

Figure 8. Local mass flux in rod bundle with various central rod APDs in Case 3 I

The variation of central rod APDs has a strong effect on the axial distribution of the mixture velocity in adjacent channels. Moreover, such effect propagates with the interaction among the open and narrow subchannels. As shown in Figure 7, the mixture mass flux in the hot central subchannels under the outlet peak distribution is notably lower than that in the cold central subchannels compared to the inlet peak distribution. The results indicate that the influence of axial power varying in T/H behavior in the channels have a certain propagative nature. However, the global extent of this effect is not significant; in Case 2 I - 3 I, the mixture mass flux or void fraction in the corner and side channels almost remain constant.

To investigate the power distribution effect on the solid region, the maximum cladding temperature $T_{clad,max}$ of different rods are also selected as one of metrics. It can be seen from Figure 9 that although the variation of the APD of the hot rod (central rod) does exert an effect on the $T_{clad,max}$ of other rods, the influence is actually very slight. Specifically, the largest $T_{clad,max}$ variation of other heating rods is only 0.48 °C, and in most cases, the $T_{clad,max}$ variations falls within the range of ± 0.3 °C. Compared to that of the central rod (the largest value is 4.4 °C, Case 1 I in Figure 9), the $T_{clad,max}$ variations of other rods resulted from central rod APD varying can be considered negligible.

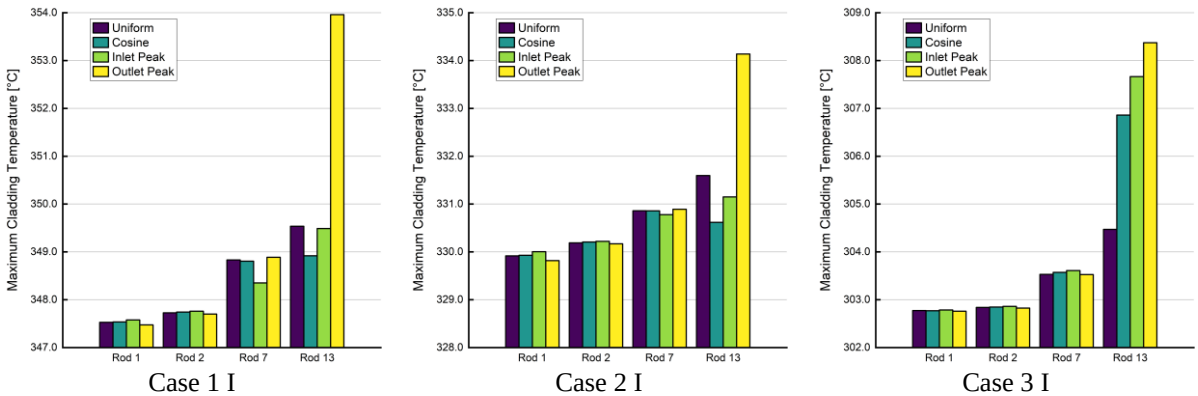

Case 1 I Case 2 I Case 3 I

Figure 9. Maximum Cladding Temperature After Different APDs Applied to Central Rod

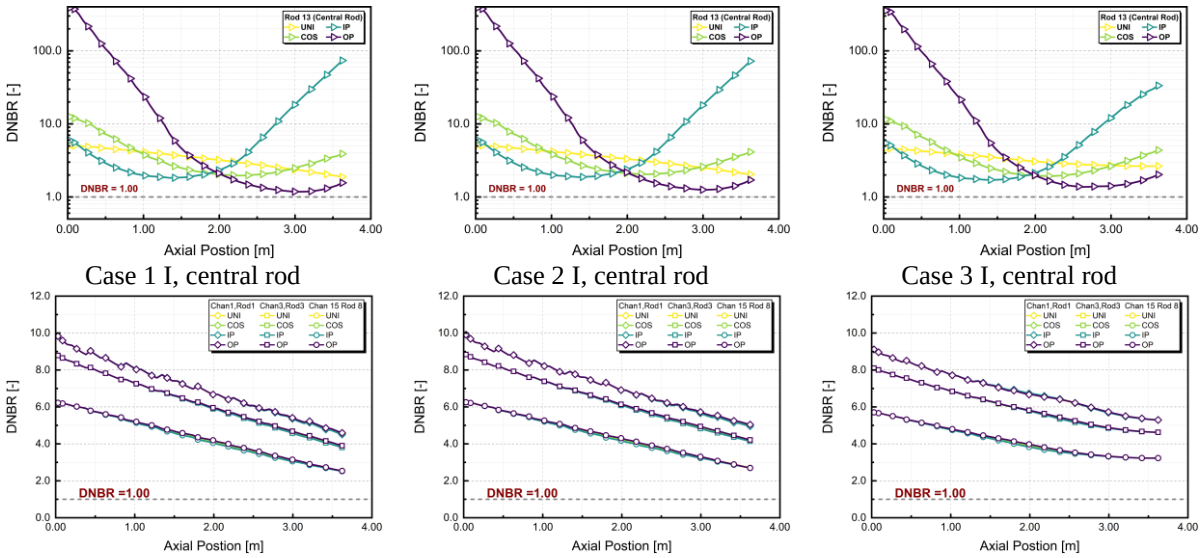

Case 1 I, central rod | Case 2 I, central rod | Case 3 I, central rod

Case 1 I, non-central rods | Case 2 I, non-central rods | Case 3 I, non-central rods

Figure 10. DNBR distribution with different central rod APDs

As a critical safety criterion for assessing the performance and safety of nuclear reactor coolant systems, the influence of APD varying in the distribution of DNBR (Departure from Nucleate Boiling Ratio) has also been studied. From Figure 10, it can be seen that the value and location of MDNBR (Minimum DNBR) on the surface of the central rod are remarkably influenced by its own axial power profile. The MDNBR location of central rod obviously shifts towards the power peak. Additionally, under outlet peak distribution, the MDNBR value decreases from 1.88 to 1.18, already below 1.3, which is a limit value under normal operating conditions and anticipated operational occurrences in PWR designs. However, the varying central rod APD has almost no effect on the MDNBR in other subchannels, regardless of the value or location. As for the DNBR distribution in axial direction, compared to the significantly changed DNBR distribution of central rod with various APDs, little variation is observed in DNBR distribution of non-central rods. This indicates that the impact of APD varying on DNBR is local.

4.3. Influence of APD patterns on T/H parameters

In this section, the influence of radial power distribution (RPD) is also considered to achieve a comprehensive assessment of the power distribution effect. That is, the power of the hot rod (central rod) gradually decreases and thereby the RPD gradually flattens to observe whether the effect of APD varying on T/H characteristics in subchannels is weakened or enhanced. Taking Case 2 as the study object, different types of RPD (I-IV) are set, as shown in Fig. 11.

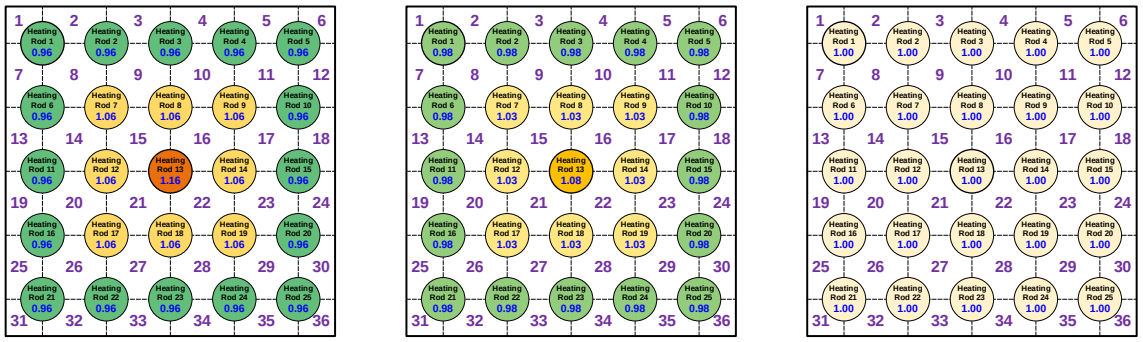

II | III | IV

Figure 11. Radial Power Distribution Patterns, from Convex to Even

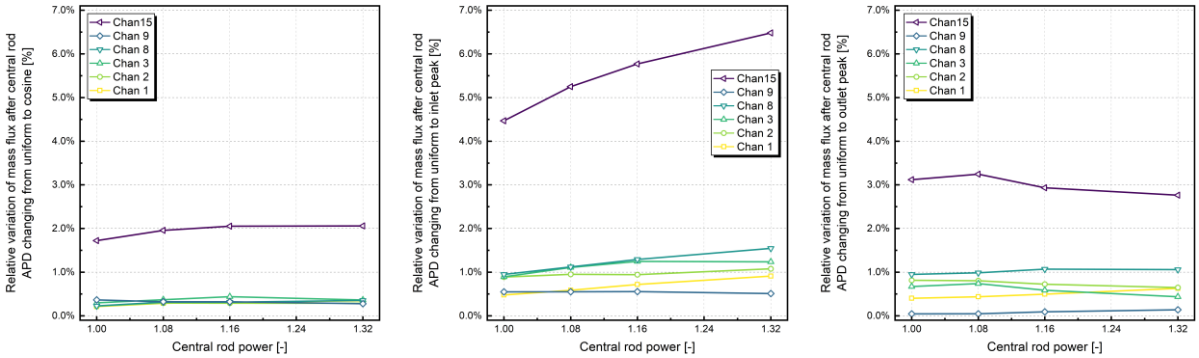

(a) (b) (c)

Figure 12. Radial Power Distribution Patterns, from Convex to Even

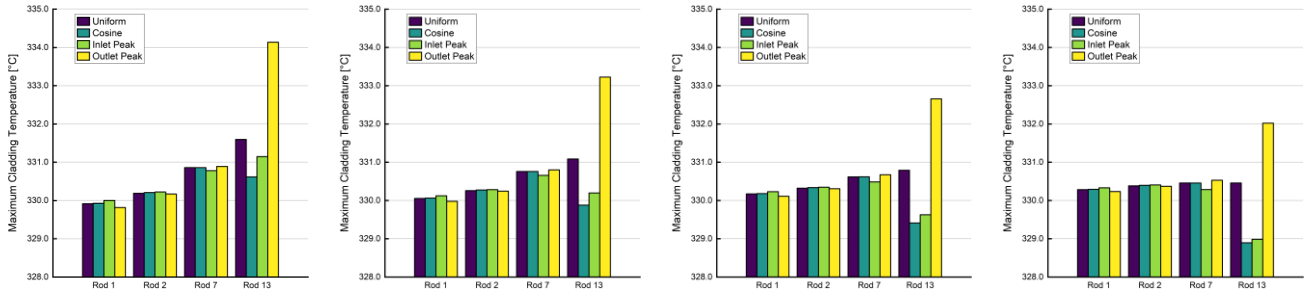

Case 2 I Case 2 II Case 2 III Case 2 IV

Figure 13. Maximum Cladding Temperature with Different RPDs And Central Rod APDs

Figure 12 illustrates the influence of central rod APD varying on the mixture mass flux in subchannels under different RPDs. It can be seen that although the radial power shape becomes more convex as the central rod power rises, the APD impact remains relatively stable rather than increases sharply. Except for channels adjacent to the central rod, the relative variations of mass flux $|\Delta G|/G$ in other channels are within 1.6%. These results indicate that the impact of axial power distribution varying is non-global, although it does propagate with interaction between subchannels. Figure 13 depicts the magnitude of the APD impact under different RPDs. It can be observed that even for a completely uniform RPD (Case 2 IV), the central rod APD varying still results in changes in other rods' cladding temperature. However, as the central rod heating power increases from 1.00 to 1.32, the maximum $T_{clad,max}$ variation of other rods does not exceed 0.1°C. Only the $T_{clad,max}$ of the central rod is changing drastically, which once again indicates the influence of APD varying on the solid temperature in rod bundle is spatially local.

5. CONCLUSION

The study investigates the impact and propagation of axial power distribution (APD) varying on the thermal-hydraulic characteristics in subchannels. The PSBT 5×5 rod bundle was taken as the research object. After model validation, taking the uniform APD as the baseline, several T/H parameters were compared under various central rods APD (uniform, cosine, inlet peak, or outlet peak distribution). Furthermore, the effect of radial power distribution (RPD) was taken into consideration to observe whether the APD impact will be amplified or diminished.

The results showed that the change of heating rod APD will significantly affect the DNBR distribution on its surface. The MDNBR value might be below the safety limit under certain APD patterns, which indicates the axial power profile is a key parameter to be considered in PWR design. The position of local hot-spot on the cladding surface and the peak cladding temperature will correspondingly shift and fluctuate. Additionally, the thermal-hydraulic behaviors in subchannels adjacent to heating rods whose APD varies will also be notably affected, such as local void fraction and coolant mass flux. However, such influence tends to manifest as a local effect. Even when the central rod APD transitions from uniform to extremely distorted shapes, the variations in void fraction and liquid-vapor mixture mass flux in side or corner subchannels remains almost unchanged. Moreover, the APD impact on solid region is limited. The variations in $T_{clad,max}$ of other rods fall within the range of ± 0.5°C. Combined analysis of axial and radial power distribution varying shows that despite the intensification of non-uniformity in RPD, the influence of APD varying and its diffusion within the

bundle do not exhibit significant changes. For instance, as the relative heating power of the central rod increases from 1.00 to 1.32, the relative variation of mass flux in other channels are only 1.6%. In general, considering both axially and radially power varying, the changes in thermal-hydraulic characteristics in rod bundle induced by single rod APD varying are local and are confined to adjacent channels rather than violently propagate within the rod bundle.

Acknowledgements

This work is supported by Lingchuang Research Project of China National Nuclear Corporation.

References

[1] Yang, Bao-Wen, Bin Han, Aiguo Liu, and Sipeng Wang. Recent challenges in subchannel thermal-hydraulics-CFD modeling, subchannel analysis, CHF experiments, and CHF prediction. Nuclear engineering and design, 354, 110236, 2019.

[2] Yang, B. CHF Mechanisms in Rod Bundle Subchannel Systems. Xi'an Jiaotong University, Xi'an, China, 2017.

[3] Yang, Baowen, Jianqiang Shan, Junli Gou, Hui Zhang, Aiguo Liu, and Hu Mao. Uniform versus nonuniform axial power distribution in rod bundle CHF experiments. Science and Technology of Nuclear Installations, 2014.

[4] Zhao, Dawei, Wenxing Liu, Wanyu Xiong, Yuanfeng Zan, and Zumao Yang. Theoretical research on DNB-type critical heat flux with non-uniform axial heat flux distribution. Nuclear Power Engineering 37, no. 1, 18-22, 2016.

[5] Zhu, Gan, and Heng Xie. Subchannel analysis of critical heat flux in radially Non-uniform heated rod assembly at low flow rate. Annals of Nuclear Energy, 180, 109446, 2023.

[6] Wang, Sipeng, Bao-Wen Yang, Hu Mao, Yu-chen Lin, and Guanyi Wang. "The influence of non-uniform heating on two-phase flow instability in subchannel." Nuclear Engineering and Design 345, 7-14, 2019.

[7] Dai, Zhiwen, Chenglong Wang, Dalin Zhang, Wenxi Tian, Suizheng Qiu, and G. H. Su. Impact of axial power distribution on thermal-hydraulic characteristics for thermionic reactor. Nuclear Engineering and Technology 53, no. 12, 3910-3917, 2021.

[8] Thurgood, M. J., J. M. Kelly, K. L. Basehore, and T. L. George. COBRA-TF: a three-field two-fluid model for reactor safety analysis. In Experimental and analytical modeling of LWR safety experiments, presented at the national heat transfer conference, 19th, 1980. 1980.

[9] Rao, Y. F., Z. Cheng, G. M. Waddington, and A. Nava-Dominguez. ASSERT-PV 3.2: advanced subchannel thermalhydraulics code for CANDU fuel bundles. Nuclear Engineering and Design, 275, 69-79, 2014.

[10] Liang, Yu, Dalin Zhang, Jing Zhang, Xiao Liu, Yapeng Liu, Lei Zhou, Yutong Chen et al. A subchannel analysis code SACOS-Na for sodium-cooled fast reactor. Progress in Nuclear Energy, 166, 104959, 2023.

[11] Salko, Robert, Aaron Wysocki, Taylor Blyth, Aysenur Toptan, Jianwei Hu, Vineet Kumar, Chris Dances et al. CTF: A modernized, production-level, thermal hydraulic solver for the solution of industry-relevant challenge problems in pressurized water reactors. Nuclear Engineering and Design 397, 111927, 2022.

[12] Salko Jr, Robert, Aaron Wysocki, A. Toptan, Nathan Porter, Xingang Zhao, Belgacem Hizoum, Taylor S. Blyth et al. CTF Validation and Verification: Version 4.4. No. ORNL/SPR-2023/3140. Oak Ridge National Laboratory (ORNL), Oak Ridge, TN (United States), 2023.

[13] Salko Jr, Robert, Maria Avramova, Aaron Wysocki, Belgacem Hizoum, Aysenur Toptan, Jianwei Hu, Nathan Porter et al. CTF Theory Manual: Version 4.3. No. ORNL/SPR-2022/2494. Oak Ridge National Laboratory (ORNL), Oak Ridge, TN (United States), 2023.